Proton and electron precipitation over Svalbard - first results from a new Imaging Spectrograph (HiTIES)

B. S. Lanchester[1], M. H. Rees[1], S. C. Robertson[1], D. Lummerzheim[2], M. Galand[3], M. Mendillo[3], J. Baumgardner[3], I. Furniss[4], and A. D. Aylward[4]

[1]University of Southampton, U.K.
[2]Geophysical Institute, University of Alaska, Fairbanks
[3]Center for Space Physics, Boston University, Boston, Massachusetts
[4]University College London, U.K.

Proton and electron precipitation over Svalbard - first results from a new Imaging Spectrograph (HiTIES)

B. S. Lanchester[1], M. H. Rees[1], S. C. Robertson[1], D. Lummerzheim[2], M. Galand[3], M. Mendillo[3], J. Baumgardner[3], I. Furniss[4], and A. D. Aylward[4]

[1]University of Southampton, U.K.
[2]Geophysical Institute, University of Alaska, Fairbanks
[3]Center for Space Physics, Boston University, Boston, Massachusetts
[4]University College London, U.K.

Abstract. An unusually intense energetic proton precipitation event occurred on 26 November 2000. The resulting surface brightness of Hydrogen beta amounted to several hundred Rayleighs. This made it possible to examine the line profile at 1.3 Å resolution in 60 s exposures for several hours in the magnetic zenith, a combination of spectral and temporal resolution not previously achieved. We confirm the existence of a significant red-shifted component, the result of upward flowing emitting hydrogen atoms. The N_2^+ 1N (1,3) filter showed, in addition to the nitrogen ion band, several lines of the atomic oxygen ion of the (^{4}P–^{4}D) multiplet 1. The Doppler profile indicates that the incident proton spectrum must have been in the range of a few hundred eV to perhaps a few keV energy, a conjecture corroborated by near-coincident (in time and space) measurements of proton spectra from the DMSP F12 and FAST satellites.

1 Introduction

A new instrumental platform has been installed at Longyearbyen on Svalbard (78.9°N, 15.8°E) to study the auroral emissions produced by precipitating protons and electrons in the region of the cusp. During a campaign in November 2000, the first measurements were made of hydrogen emissions caused by precipitating protons, in the wavelength range 4844–4876 Å, covering the profile of the Balmer-β line. The event of 26 November 2000 was measured in the solar wind by the ACE and WIND spacecraft, which detected sharp increases in proton number density and velocity. The resulting precipitation over Svalbard was measured by several instruments, and data from these form the background to detailed measurements made by HiTIES (High Throughput Imaging Echelle Spectrograph).

Fig. 1 shows the ultraviolet Lyman-α emission from the Imager for Magnetopause-to-Aurora Global Exploration (IMAGE) at 14:40 UT. This emission, like the Balmer-β (H$_\beta$)

Correspondence to: B. S. Lanchester, bsl@soton.ac.uk

emission, is a signature of proton precipitation into the atmosphere (Frey et al., 2001). In Fig. 1 there is a bulge of proton precipitation south of Svalbard, with its centre close to the north coast of Norway. Super-imposed on this image is the track of the DMSP F12 satellite, passing to the north of Svalbard, but intersecting the proton precipitation region further south. The field of view of Meridian Scanning Photometers (MSP) located with the HiTIES instrument at Longyearbyen scans through this region. The MSP measures the brightness of lines and bands with tilting interference filters. This allows the background brightness in the vicinity of an emission feature to be monitored continuously, and the line brightness to be corrected by subtracting the background. This is of particular importance for the H$_\beta$ brightness, since the background brightness (e.g. from N_2 Vegard-Kaplan bands) can be comparable to, and show as much variability as the line brightness itself.

The data from the MSP are shown in Fig. 2 for 8 hours during this event. Auroral emissions are visible in all but the H$_\beta$ panel during the short 'daylight' hours, when the sun is less than 10° below the horizon, corresponding to a shadow height of about 100 km in the zenith. The N_2^+ 1N at 4278 Å and OI at 8446 Å show that structured aurora was present during the time that the H$_\beta$ was overwhelmed by scattered sunlight. There is a concurrent increase in emissions at 5577 Å and 8446 Å, but little in 6300 Å. After the onset of darkness near 13:00 UT there is continuing precipitation of H$_\beta$ until about 16:00 UT. The OI emissions at 6300 Å increased at the start of this interval. Between 15:00 and 15:15 UT more than 250 R of H$_\beta$ is measured, mostly to the south of Longyearbyen.

Particle spectra from the DMSP satellite F12 and F13 are available for times close to the proton event, with passes that intersect the precipitation region close to Svalbard at 14:39 UT and 14:07 UT respectively. The spectra from the two passes are similar at these times. The incident flux is largest at energies of 1-2 keV with a high energy tail beyond the cutoff of the instrument at 30 keV. Soft electrons are collocated with the energetic protons. The observing geometry
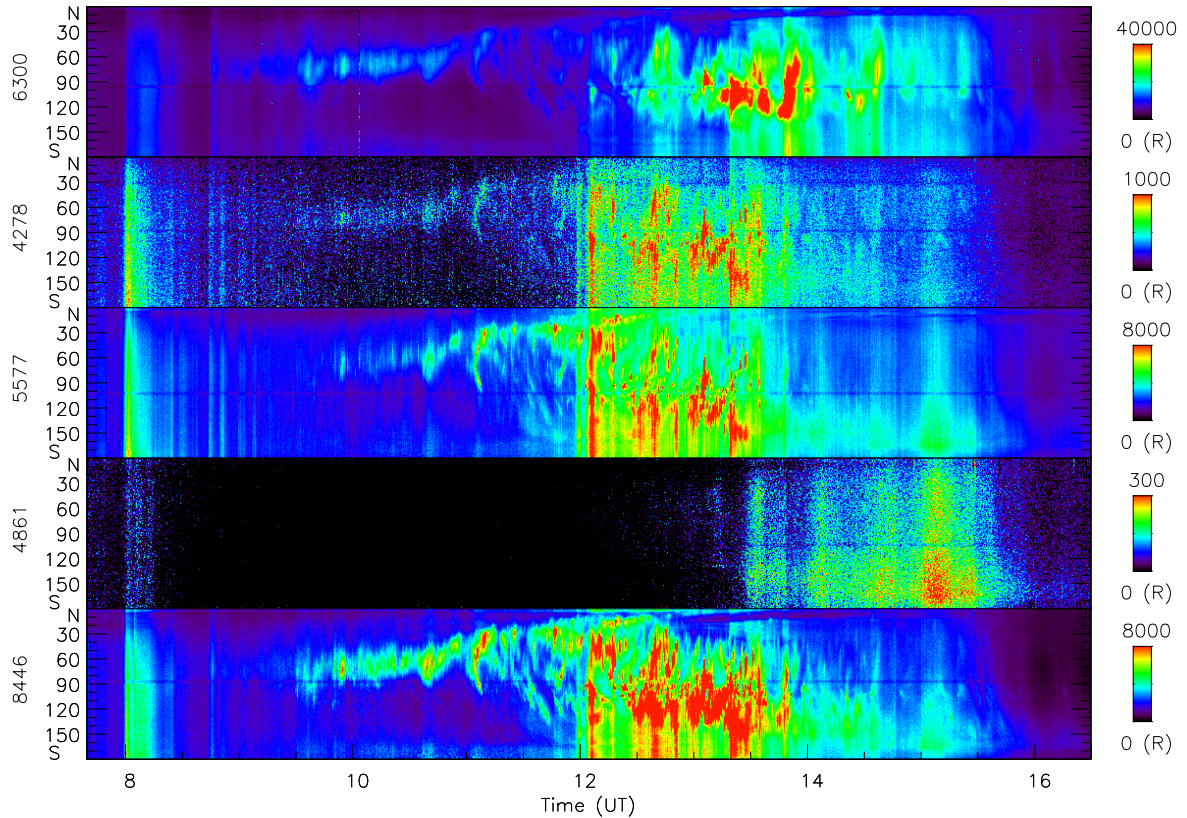
Fig. 2. Data from the Svalbard Meridian Scanning Photometers. Each panel shows the auroral brightness as a function of meridian scan angle and time. The wavelengths shown are (top to bottom) OI(6300 Å), N_2^+ 1N(4278 Å), OI(5577 Å) H_β(4861 Å), OI(8446 Å.

of the FAST satellite is better than that of the DMSP satellites, with closest approach to Longyearbyen at 15:28 UT. Protons of 1-2 keV are measured over Longyearbyen, also with a high energy tail to the energy spectrum. Further equatorward, in the region of intense proton precipitation (seen by IMAGE), increased fluxes with higher energies are measured by FAST, but it appears that most of the particle flux could be above the detector upper threshold of 30 keV.

2 Imaging Spectrograph

The High Throughput Imaging Echelle Spectrograph (HiTIES) is described in Baumgardner et al. (1993) and elsewhere in these proceedings (McWhirter et al. (2002)). The data recorded to date have demonstrated that the imaging spectrograph is capable of measuring auroral emissions, in particular H_β, with high spectral resolution ($\sim$1.3 Å) and high time resolution ($<$1 min). The field of view is a narrow slit of $8°$ centred on the magnetic zenith. The data shown here have been integrated over the central $6°$ of the slit, which for H_β emission has the effect of increasing the signal without any loss of information. Changing this angle does not

affect significantly the magnetic zenith profiles.

In addition to the H_β spectral window, two others were chosen on this campaign, to measure the N_2^+ 1N bands (4635–4660 Å) and (4690–4715 Å). They are shown in Fig. 3 and Fig. 4. In order to identify features the spectra have been co-added in time from 13:00-14:20 UT. An observation that was not anticipated is the presence of three lines of a multiplet of OII in the pass-band of the filter selected for the N_2^+ 1N (1,3) band (4651.8 Å) shown in Fig. 3. In addition, there is an unidentified emission near 4645 Å. The emission OII 4649.1 Å overlaps the N_2^+ 1N (1,3), but by fitting a synthetic spectrum to the 1N band, the two features can be separated. A sample synthetic spectrum assuming a neutral temperature of 1500 K is superimposed in Fig. 3 (thin line). This is constructed from synthetic molecular band profiles using the model of Degen (1977). The synthetic spectrum was convolved with the HiTIES instrument function representing a resolution of 1.3 Å. Fig. 4 shows the spectral window for N_2^+ 1N (4709 Å), with several rotational lines visible. This band shape is reproduced quite well by fitting of a synthetic spectrum for 1500 K, but detailed analysis has still to be made. Individual spectra taken at 1 min resolution have enough definition to deduce the rotational temperature,
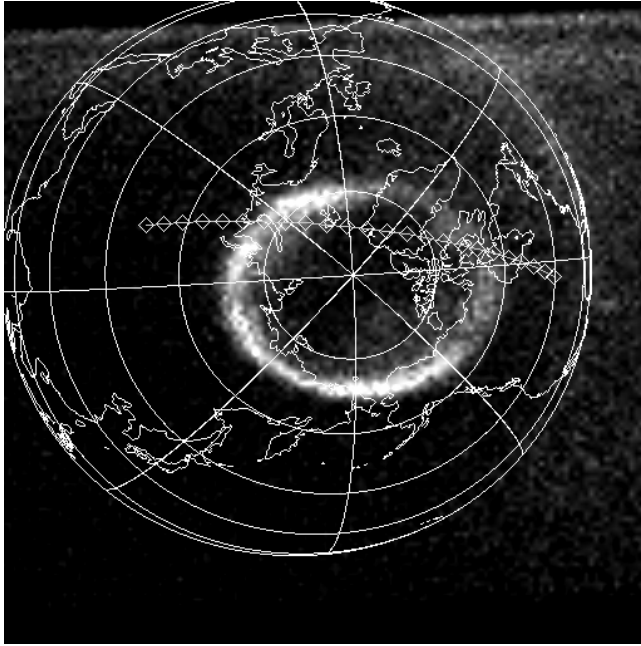
equivalent to the kinetic temperature.

The imaging spectrograph acquires H_β line profiles at a combination of spectral and temporal resolution not previously achieved. Fig. 5 is a sample of these data from two times of bright hydrogen emission over Longyearbyen at 60 s resolution. The background brightness obtained from the spectral region longward of the H_β line has been subtracted from the data. Notable features of these profiles are:

a) The shape of the two profiles changes through the event, seen mainly in the raised wing at shorter wavelengths. The greater the intensity at shorter wavelengths, the larger the flux of high energy protons in the incoming energy spectrum. (Note that possible contamination from molecular bands has not yet been subtracted.)

b) The red-shifted wing is a real and significant feature of these data, indicating the presence of back-scattered hydrogen atoms. The red shift is greater than the width of the instrument function (1.3 Å).

c) The peak of the profile varies in wavelength from the unshifted hydrogen line at 4861.3 Å. As the blue-shifted wing decreases with time, so the peak appears to move to longer wavelengths. This shows that the profile at 15:07:22 UT was produced by a proton flux of much lower mean energy than at 13:33:01 UT.

3 Modelling

The shape and shift of these profiles can only be explained theoretically by modelling the complex processes of atomic physics leading to the emission profile. The model we have used solves the proton-hydrogen transport equations, allow-
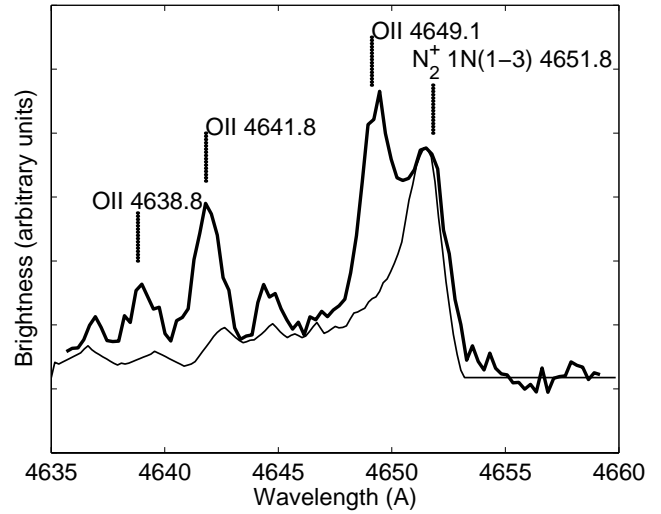
Fig. 3. Spectrum from the HiTIES instrument (magnetic zenith) integrated from 13:00-14:20 UT. Auroral emission features are indicated. A synthetic spectrum of N_2^+ 1N with neutral temperature of 1500 K (thin line) is superimposed.
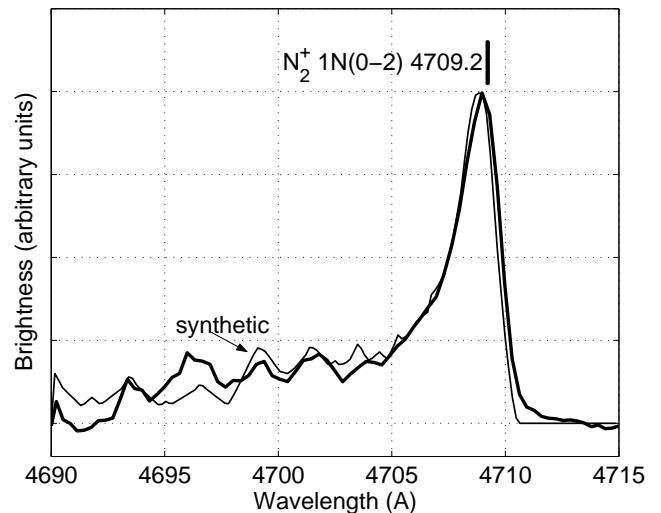

Fig. 4. Spectrum of the spectral window (magnetic zenith) for N_2^+ 1N (4709 Å) integrated from 13:00-14:20 UT. A synthetic spectrum of N_2^+ 1N with neutral temperature of 1500 K is superimposed.
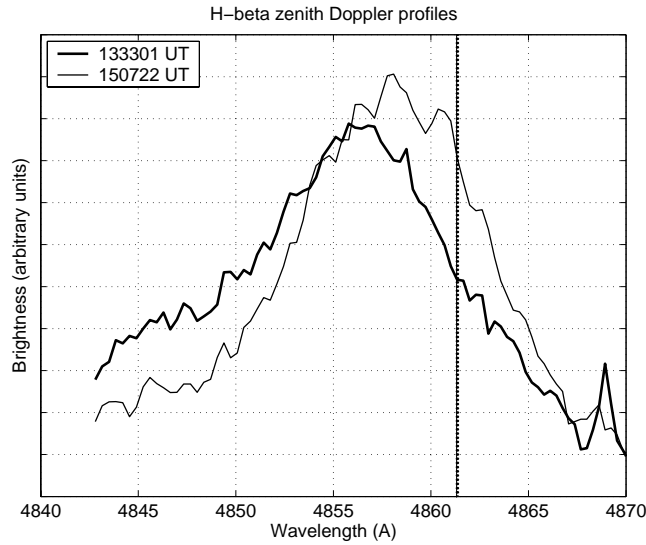
Fig. 5. Spectrum of the H_β line spatially integrated over $6°$ in the magnetic zenith at 13:33:01 UT and 15:07:22 UT). The background brightness is subtracted. The unshifted wavelength is at 4861.3 Å. The blue shifted component results from the line of sight velocity of downward moving hydrogen. The red shifted wing is the consequence of upward moving hydrogen.

Fig. 6. Modelled H_β line profile along the magnetic zenith, including angular redistribution in the transport of the precipitating H/H$^+$ stream. The dashed line shows the theoretical line profile, the solid line is the same profile after convolution with the HiTIES instrument function. The rest wavelength is indicated by the dotted line.

ing for charge-exchange, stripping, ionisation, excitation, and elastic collisions (Galand et al., 1998). It is one-dimensional along the magnetic field direction. Fig. 6 shows the preliminary result using as input the ion energy spectrum from the DMSP pass between 14:39:03 and 14:39:07 UT. There are significant differences between the modelled and measured H_β profiles, which is not surprising, given the limitations of the input spectrum and approximations and assumptions of the model. The satellite pass is not an exact field-line coincidence, and the energy range of the satellite detectors is limited from 30 eV to 30 keV. The high-energy tail of the distribution has been extrapolated using results from the Proton I rocket (Söraas, 1974) to give the slope of the spectrum at high energies. This experiment was on the nightside, and therefore not necessarily appropriate here. Further modelling work is needed. The red-shifted wing is well reproduced and is evidence that there are back-scattered hydrogen atoms present, although there is a greater red-shifted contribution than predicted by the model. The same model was used in work by Lummerzheim and Galand (2001) who found agreement between the red shift of H_β profiles observed on the nightside oval and modelled profiles. The cross-sections used are the same as in (Galand et al., 1998), with the assumption of collisional angular redistribution below 50 keV, and with the elastic cross-sections for O_2 and O assumed to be equal to that of N_2.

The observed changes to the peak of the profiles in the present dayside observations have not yet been reproduced with the model. The model predicts that, at high spectral resolution, the blue shift of the peak changes only by small amounts for different proton mean energies, while the width of the blue-shifted wing of the emission changes more dramatically (Lummerzheim and Galand, 2001). Spectra from
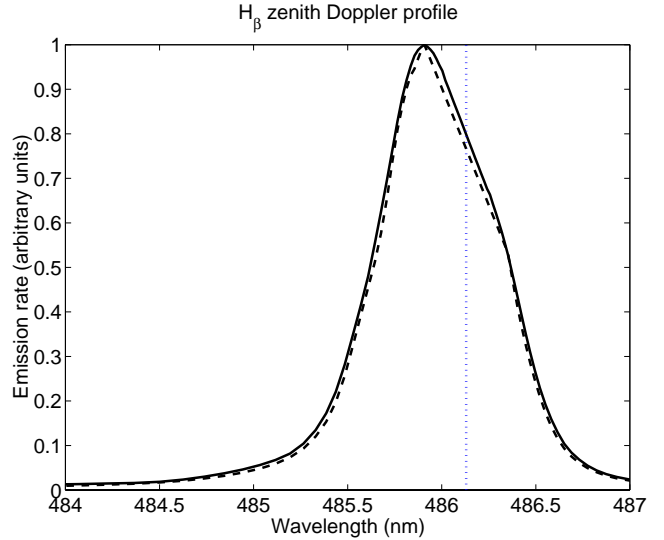
different times as seen in Fig. 5 show a similar behaviour and are likely to be caused by proton precipitation with different mean energies and with angular distributions different from the isotropic distribution assumed in the model. The shift of the peak from model predictions is slightly smaller than the observed shift (by about 1-2 Å).

References

Baumgardner, J., B. Flynn, and M. Mendillo, Monochromatic imaging instrumentation for applications in aeronomy of the earth and planets, Optical Eng., 32, 3028-3032, 1993.

Degen, V., Modeling of N_2^+ First Negative spectra excited by electron impact, *J. Quant. Spectroscopic Radiat. Transfer*, *18*, 113–119, 1977.

Frey, H. U., S. B. Mende, C. W. Carlson, J.-C. Gerard, B. Hubert, J. Spann, R. Gladstone, and T. J. Immel, The electron and proton aurora as seen by IMAGE-FUV and Fast, *Geophys. Res. Lett.*, *28*, 1135–1138, 2001.

Galand, M., J. Lilensten, W. Kofman, and D. Lummerzheim, Proton transport model in the ionosphere: 2, Influence of magnetic mirroring and collisions on the angular redistribution in a proton beam, *Ann. Geophys.*, *16*, 1308, 1998.

Lummerzheim, D. and M. Galand, The profile of the hydrogen H_β emission line in proton aurora, *J. Geophys. Res. 106*, 23–31, 2001.

McWhirter, I., I. Furniss, A.D. Aylward, B.S. Lanchester, M.H. Rees, S.C. Robertson, J. Baumgardner, and M. Mendillo, A new spectrograph platform for auroral studies in Svalbard, *Proc. Atmospheric Studies by Optical Methods*, Oulu, 2001, this issue.

Söraas, F., H. R. Lindalen, K. Måseide, A. Egeland, T. A. Sten, and D. S. Evans, Proton precipitation and the H_β emission in a postbreakup auroral glow, *J. Geophys. Res. 79*, 1851–1859, 1974.